Electromagnetic–Thermal Coupling Analysis of an Outer-Rotor I-Shaped Flux-Switching Permanent-Magnet Motor Considering Driving Cycles

Chang Liu, Xiaoyong Zhu, Li Quan, Zixuan Xiang, Xue Wang, Juan Huang

School of Electrical and Information Engineering, Jiangsu University, Zhenjiang, 212013 China, zxyff@ujs.edu.cn

This paper presents a lumped parameter (LP) thermal method for outer-rotor I-shaped flux-switching permanent-magnet (I-FSPM) motor. Considering the EVs application, the New European Drive Cycle (NEDC) is chosen to be the sample driving cycle to predict the motor temperature characteristic. To improve the prediction accuracy, the thermal contact resistances between two different materials are considered in the proposed method. In addition, an instantaneous power loss is also calculated and analyzed during the whole driving cycle. To verify the proposed method, a 3-D finite-element (FE) method is simultaneously utilized to obtain the temperature characteristic. The theoretical analysis and calculated results reveal that the proposed method possesses a high accuracy. Finally, a prototype motor is manufactured and tested for the validity.

***Index Terms*—Flux-switching permanent-magnet motor, electromagnetic–thermal coupling, lumped parameter, driving cycles**

I. Introduction

IN RECENT decades, flux-switching permanent-magnet (FSPM) motors have been increasingly employed due to the merits of high power density and high efficiency, which are regarded as potential candidate for electric vehicles (EVs) [1]-[2]. In such motors, the PMs and armature windings are all located in the stator, where a concentrated coil is wound around each stator pole, thus resulting in a concentration of heat sources. Hence, when the motor is driving continuously, some problems will occur easily, such as the irreversible demagnetization of PM and insulation failure of coils. Thus, it is necessary to precisely predict the temperature distribution of the motor, especially in various driving cycles.

Generally, there are three kinds of methods for thermal analysis of electrical machines, namely, finite-element (FE) method, computational fluid dynamics (CFD), and lumped parameter (LP) method [3]. Yet, the FE method and CFD method are relatively time consuming, and they usually make a strict demand on hardware computing capability. Therefore, to the common researchers, a simple and efficient thermal analysis of motor is relatively difficult to be realized in such ways, especially for a complex motor structure. In recent years, the lumped parameter methods have aroused some concerns, mainly because they have the advantages of simple and fast computation. In [4], the method is adopted to investigate the temperature distribution for a FSPM motor, exhibiting a high predicted accuracy. Yet, in existing studies, the researchers mainly focus on the temperature analysis in single operation point, while it in whole driving cycle is solely involved. In EV operation, the frequent acceleration and deceleration, sudden start-stop and heavy load and hill-climbing are often required to be conducted by traction motor. And it is noted that the temperature distribution of motor is directly determined by the various driving conditions. So, it is crucial for predicting the motor temperature precisely based on the consideration during the whole driving cycle.

In this paper, a simple and fast lumped parameter thermal method is presented for outer-rotor I-shaped flux-switching permanent-magnet (I-FSPM) motor. And the New European Drive Cycle (NEDC) is adopted and served as the sample driving cycle to predict the motor temperature characteristic. In addition, a FEM transient 3-D model is also established to verify the validity. Finally, the experiments on the prototype machine are carried out to verify the accuracy of the proposed method.

II. Motor Configuration and LP Model

Fig. 1(a) illustrates the I-FSPM motor with the pole/slot combination of 22-pole rotor/12-slot stator, in which the concentrated windings and PMs are located in the stator, thus leading to a simple and robust rotor. And the basic design specifications of the rated power and speed are designed with 2kW and 800 rpm respectively.

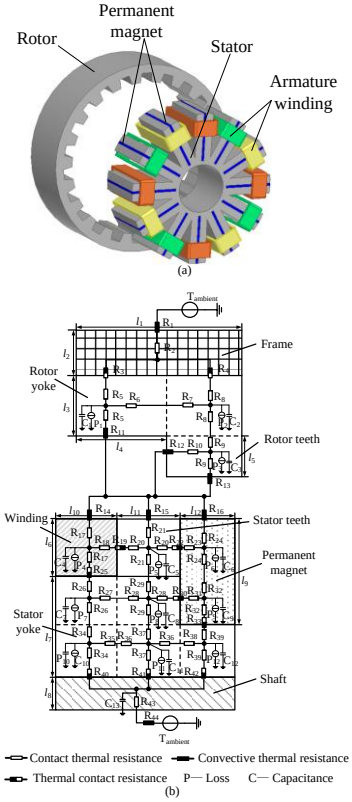

Fig. 1. (a) Configuration of the motor. (b) LP thermal model of the motor.

The LP thermal model of the motor is built, where 1/44 of the rotor and 1/24 of the stator can be modeled to obtain a simplification, as shown in the Fig. 1(b). In this paper, only the radial direction of heat conduction is considered due to the axial direction is small relative to radial direction. The contact thermal resistances are also considered except for the conductive thermal resistance and convective thermal resistance. To analyze conveniently, the designed slots are transformed into a rectangular slot shape without changing the area of the slots.

III. Loss Calculation During Driving Cycles

The New European Drive Cycle (NEDC) is chosen to investigate the thermal behavior of the motor, as shown in Fig. 2(a). Fig. 2(b) depicts the torque requirements over the NEDC for the motor. Under the load current of 11A, the copper loss over NEDC can be calculated, as shown in Fig. 2(c). The iron loss of the motor can be calculated according to the core loss model presented by Yamazaki in [5]. The model can be formulated as follows:

$$W_{ie} = \frac{K_e D}{2\pi^2}\int_{\text{iron}} \frac{1}{N}\sum_{k=1}^{N}\cdot\left\{\left(\frac{B_r^{k+1}-B_r^k}{\Delta t}\right)^2+\left(\frac{B_\theta^{k+1}-B_\theta^k}{\Delta t}\right)^2\right\}dv \quad (1)$$

$$W_{ih} = \frac{K_h D}{T}\sum_{i=1}^{NE}\frac{\Delta V_i}{2}\left(\sum_{j=1}^{N_{pr}^i}\left(B_{mr}^{ij}\right)^2+\sum_{j=1}^{N_{p\theta}^i}\left(B_{m\theta}^{ij}\right)^2\right) \quad (2)$$

where D is the density of the core, N is the number of time step per one time period, Δt is the time interval, ΔV_i is the volume of i^{th} finite element. B_{mr} and $B_{m\theta}$ are the amplitude of each hysteresis loop. K_e and K_h can be obtained by experimental loss cures based on polyfit method. Then iron loss can be calculated, as shown in Fig. 2(d).

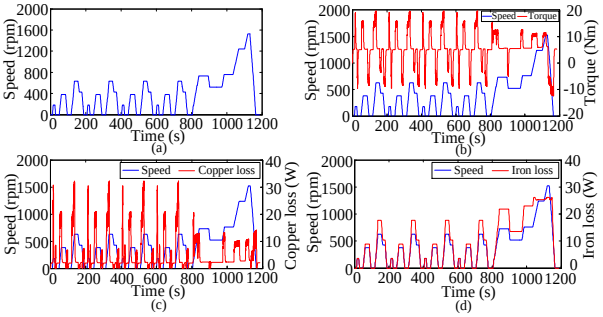

Fig. 2. (a) NEDC. (b) Torque requirements over NEDC. (c) Copper loss over NEDC. (d) Iron loss over NEDC.

IV. Thermal Analysis and Experimental Validation

After loss calculation, the thermal analysis is conducted based on the LP thermal model and FEM 3D transient model. And based on the NEDC, an average loss is used as the heat sources, which is obtained from eight driving conditions. Considering the risks of PM demagnetization and insulation failure of coils, a special consideration is taken into the temperature of armature winding and PM, and their transient temperature using average losses are illustrated in Fig. 3(a). It can be seen that the maximum temperature of the winding in LP thermal model is about 67.6°C, while that in FEM transient 3D model is about 65°C, indicating a highly closed prediction results. Similary, the temperature of the PMs in the two prediction ways also exhibit a desirable coincidence between them, which respectively reach the values of 62.2°C and 60.3°C. For better presentation, the transient temperature of the motor using calculated instantaneous losses by LP thermal model is also calculated, as shown in Fig. 3(b). From the figure, the maximum temperature of the winding is about 69°C, which is higher than the results in Fig. 3(a). And the maximum temperature of the PM using instantaneous losses is about 76°C, which is also higher than it calculated with the average losses. Based on the above invesigation, it infers that, compared with the situation of average losses, the temperature analysis with the instantaneous losses is more accorded with a actual motor operation and has a higher reference value.

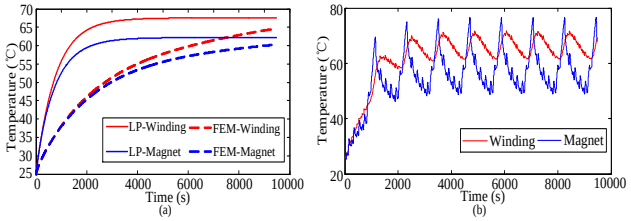

Fig. 3. (a) Transient temperature of motor winding and magnets using average losses. (b) Transient temperature of motor winding and magnets using instantaneous losses by the LP model.

To testify the validity of the proposed LP thermal model, the prototyped machine is manufactured, as shown in Fig. 4(a). And Fig. 4(b) and Fig. 4(c) display the experimental platform and the measured back-EMF waveform respectively. The measured steady-state torque and current waveforms of the motor are shown in Fig. 4(d). More detailed thermal analysis and experiment results will be given in the full paper.

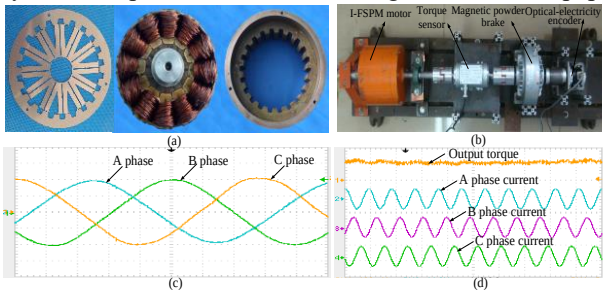

Fig. 4. (a) Prototype of the motor. (b) Experimental platform. (c) Measured back-EMF waveform (18V/div, 1.25ms/div). (d) Measured steady-state torque and current waveforms.

References

[1] M. Cheng, W. Hua, J. Z. Zhang, and W. X. Zhao, "Overview of stator permanent magnet brushless machines," *IEEE Trans. Ind. Electron.*,vol. 58, no. 11, pp. 5087–5101, Nov. 2011

[2] R. W. Cao, C. Mi, and M. Cheng, "Quantitative comparison of flux-switching permanent-magnet motors with interior permanent magnet motor for EV, HEV, and PHEV applications," *IEEE Trans. Magn.*,48(8), pp. 2374–2384, 2012.

[3] A. Boglietti, A. Cavagnino, and D. Staton, "Determination of critical parameters in electrical machine Thermal Models," *IEEE Trans. Ind. Appl.*, vol. 44, no. 4, July./Aug. 2008.

[4] X. H. Cai, M. Cheng, and S. Zhu, "Thermal modeling of flux-swiching permanent magnet machines considering anisotropic conductivity and thermal contact resistance," *IEEE Trans. Ind. Electronics.*, vol. 63, no. 6, June. 2016.

[5] K. Yamazaki, "Torque and efficiency calculation of an interior permanent magnet motor considering harmonic iron losses of both the stator and rotor ," *IEEE Trans. Magn.*, vol. 39, no. 3, May. 2003.